



Optical Properties of Novel 2,3-Dicyano-5-methyl-6*H*-1,4-diazepine Dyes in the Solid State

Emi Horiguchi, Shinya Matsumoto,¹ Kazumasa Funabiki, and Masaki Matsui*

Department of Materials Science and Technology, Faculty of Engineering, Gifu University, Yanagido, Gifu 501-1193

¹Department of Environmental Sciences, Faculty of Education and Human Sciences, Yokohama National University, 79-2 Tokiwadai, Hodogaya-ku, Yokohama 240-8501

Received November 26, 2004; E-mail: matsui@apchem.gifu-u.ac.jp

Novel nonplanar fluorescent dyes, 2,3-dicyano-7-methyl-6*H*-1,4-diazepines, were synthesized. The fluorescence intensity of 6-substituted 2,3-dicyano-5-[4-(diethylamino)styryl]-7-methyl-6*H*-1,4-diazepines in vapor-deposited film was on the order of the substituent at the 6-position: *n*-Bu, Et > *t*-Bu, H. That of 2,3-dicyano-5-[4-(dialkylamino)styryl]-6-ethyl-7-methyl-6*H*-1,4-diazepines in the solid state was on the order of the alkyl group: CH₂(3,5-(di-*t*-Bu)C₆H₃) > Bn > Et. Thus, the fluorescence intensity in the solid state basically increased with the bulkiness of the substituents on the chromophoric system. X-ray structure analysis clearly showed that the substituent at the 6-position and the dialkylamino moiety should inhibit intermolecular interactions between the chromophores so as to enhance the fluorescence intensity in the solid state.

Organic electroluminescent (EL) devices have been intensively studied for use in upcoming flat panel displays (FPD), since they provide superior display characteristics, e.g. vivid image production based on a high contrast ratio, a fast imaging response, and low electricity consumption, compared with typical FPDs, such as a liquid-crystal display and a plasma display.¹ Two types of organic materials have been applied to EL devices as an emitter: low-molecular-weight organic dyes and fluorescent polymers. The conventional EL devices using organic dyes as an emitter consist of electron-transport materials, emitters, hole-transport materials, and electrodes. Three kinds of emitters for the primary colors (red, green, and blue) are required for full-colored EL devices. Among them, red emitters have usually been prepared with dopants.¹ Only fewer kinds of red emitters without dopants have been known: tetracenes,² pyrenes,³ perylenes,⁴ arylaminofumaronitriles,⁵ maleimides,⁶ and azomethine dyes.⁷ When red emitters are used without dopants, the close stacking of molecules in the solid state should bring about a decrease in the EL intensity due to intermolecular interactions. The introduction of bulky substituents into a fluorophore was considered to prevent this interference to enhance the emission intensity. A great number of materials researches have devoted efforts to develop EL characteristics; in contrast, there are only several reports on fundamental studies of the correlation among molecular structure, solid-state structure and fluorescent properties in the solid state.⁸ Thus, the molecular design for solid-state fluorescent materials is still uncertain compared to the remarkable progress in device technologies. We have proposed a novel dicyanodiazepine chromophore as a nonplanar fluorophore.⁹ The methylene moiety of 2,3-dicyano-6*H*-1,4-diazepines was found to project out of the conjugated planar π -plane. The correlation between the crystal structure of 6-substituted 2,3-dicyano-5-[4-(diethylamino)styryl]-7-methyl-6*H*-1,4-diazepines

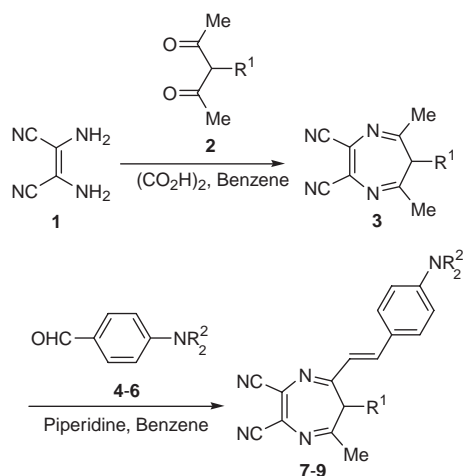
and the fluorescence intensity in the solid state was briefly reported in a previous paper.¹⁰ The introduction of bulky substituents at the 6-position was found to prohibit cofacial molecular stacking in the solid state, so that the fluorescence was not quenched, even in vapor-deposited films. In this paper, substituent effects in 2,3-dicyano-6*H*-1,4-diazepine dyes on the optical properties both in solution and in the solid state are described in detail. Special attention is paid to the correlation between the fluorescence intensity in the solid state and molecular stacking.

Results and Discussion

Synthesis of 2,3-Dicyano-5-methyl-6*H*-1,4-diazepine Dyes. The synthesis of 2,3-dicyano-5-methyl-6*H*-1,4-diazepine dyes **7–9** is shown in Scheme 1. Diaminomaleonitrile (**1**, DAMN) reacted with 3-substituted pentane-2,4-diones **2** to give 6-substituted 2,3-dicyano-5,7-dimethyl-6*H*-1,4-diazepines **3**, followed by condensation with aromatic aldehydes **4–6** to provide **7–9** in low-to-moderate yields.

Optical Properties of 2,3-Dicyano-5-methyl-6*H*-1,4-diazepine Dyes in Solution and in the Solid State. The UV–vis absorption and fluorescence spectra of **7a–d**, **8**, and **9** in chloroform are shown in Figs. 1 and 2, respectively. Their characteristics are summarized in Table 1. No significant difference was observed in the absorption maxima (λ_{max}) and fluorescence maxima (F_{max}), since the electronic structure in the visible region is only slightly influenced by substituents R¹ and R². The dyes **7a–c**, **8**, and **9**, except for **7d**, showed a λ_{max} of around 490–498 nm with a molar absorption coefficients (ϵ) of 40100–43300 dm³ mol^{−1} cm^{−1}. Their F_{max} values were observed at around 586–608 nm. In the case of **7d**, λ_{max} and F_{max} exhibit a small bathochromic shift compared with those of other derivatives. This result is attributed to the difference in the dominant stereo-isomer between **7d** and the other deriv-

atives, as discussed in a later section. However, the fluorescence intensity is quite different. A quantum yield for **7a** was calculated to be 0.03. The relative fluorescence intensity (RFI) was in the following order: **7a** \gg **9**, **7b**, **7c** $>$ **8**, **7d**. This



R^1 : **2a**, **3a** = H, **2b**, **3b** = Et, **2c**, **3c** = *n*-Bu, **2d**, **3d** = *t*-Bu
 R^2 : **4** = Et, **5** = Bn, **6** = $\text{CH}_2(3,5\text{-di-}t\text{-Bu})\text{C}_6\text{H}_3$
7a: R^1 = H, R^2 = Et, **7b**: R^1 = Et, R^2 = Et, **7c**: R^1 = *n*-Bu, R^2 = Et, **7d**: R^1 = *t*-Bu, R^2 = Et, **8**: R^1 = Et, R^2 = Bn,
9: R^1 = Et, R^2 = $\text{CH}_2(3,5\text{-di-}t\text{-Bu})\text{C}_6\text{H}_3$

Scheme 1.

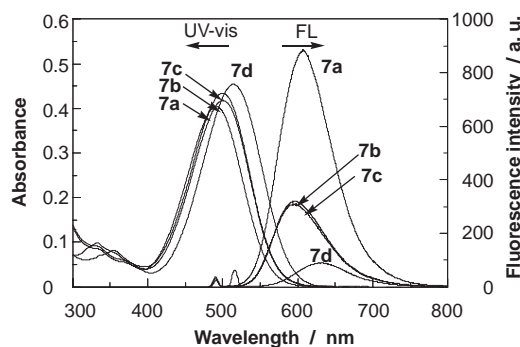


Fig. 1. UV-vis absorption and fluorescence spectra of **7a-d** (1×10^{-5} mol dm $^{-3}$) excited with the absorption maximum in chloroform.

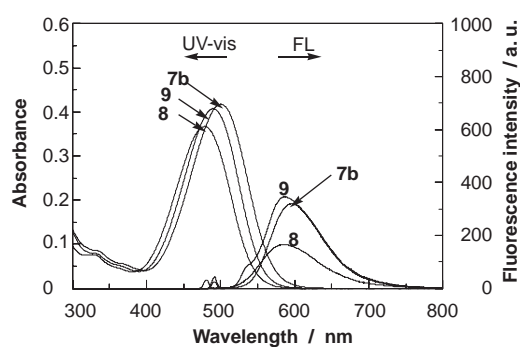


Fig. 2. UV-vis absorption and fluorescence spectra of **7b**, **8**, and **9** (1×10^{-5} mol dm $^{-3}$) excited with the absorption maximum in chloroform.

Table 1. UV-vis Absorption and Fluorescence Properties of **7-9**

Compd	R^1	R^2	CHCl $_3$ ^{a)}				Film				
			λ_{max} (ϵ_{max}) /nm	F_{max} ^{b)} /nm	RFI ^{c)}	SS ^{d)}	λ_{max} /nm	F_{max} ^{b)} /nm	RFI ^{e)}	SS ^{d)}	Thickness /nm
7a	H	Et	490 (40400)	608	100 ^{f)}	118	499	663	100	164	44
7b	Et	Et	498 (41700)	596	36	98	530	676	679	146	42
7c	<i>n</i> -Bu	Et	498 (43300)	595	35	97	551	664	860	113	40
7d	<i>t</i> -Bu	Et	514 (46800)	632	10	92	526	682	119	156	57
8	Et	Bn	479 (40100)	586	19	107	493	640	849	147	49
9	Et	$\text{CH}_2(3,5\text{-di-}t\text{-Bu})\text{C}_6\text{H}_3$	490 (41900)	587	39	97	478	637	1132	159	40

a) Measured at the concentration of 1.0×10^{-5} mol dm $^{-3}$ at 25 °C. b) Excited with the absorption maximum. c) Relative fluorescence intensity was determined by considering the fluorescence intensity of **7a** in chloroform as 100. d) Stokes Shift. e) Relative fluorescence intensity was determined by considering the fluorescence intensity of **7a** on film as 100. f) Quantum yield was calculated to be 0.03.

could be attributed to the introduction of a flexible substituents that can accelerate the internal conversion so as to reduce the fluorescence intensity in solution.¹⁰

Figures 3(A) and (B) depict the UV-vis absorption and fluorescence spectra of **7-9** in vapor-deposited thin films, respectively. Their characteristics are also listed in Table 1. The λ_{max} values were observed at around 478–551 nm, being relatively bathochromic compared with those in chloroform. The F_{max} values were observed in the range of 637–682 nm, being more bathochromic compared with those in chloroform. Even though the thickness (40–57 nm) and the absorbance (0.47–0.55) of the films were almost similar, the fluorescence intensity changed considerably: **9** $>$ **8**, **7c** $>$ **7b** \gg **7d**, **7a**, being of different order from that in solution. This change in the fluorescence intensity should be affected by intermolecular interactions in the solid state. Therefore, an attempt to analyze their crystal structure was made in order to investigate the difference in the fluorescence intensity between in solution and in the solid state.

Stacking of Molecules in Crystals. A crystal-structure analysis was carried out for **7a-c** and **8**. Unfortunately, no suitable single crystal was obtained for **7d** and **9**. A detailed examination of the crystal structures made it clear that there are three kinds of characteristic molecular pairs, as shown in Figs. 4–6: stacking pairs between phenylene rings, between di-cyanodiazepine moieties, and between whole chromophores.

Figure 4 shows the stacking pairs between the phenylene

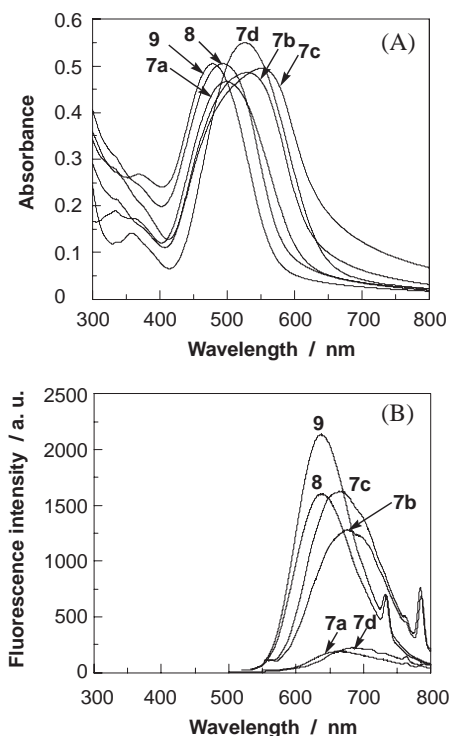


Fig. 3. (A) UV-vis absorption and (B) fluorescence spectra of **7**–**9** excited with the absorption maximum in vapor-deposited thin film.

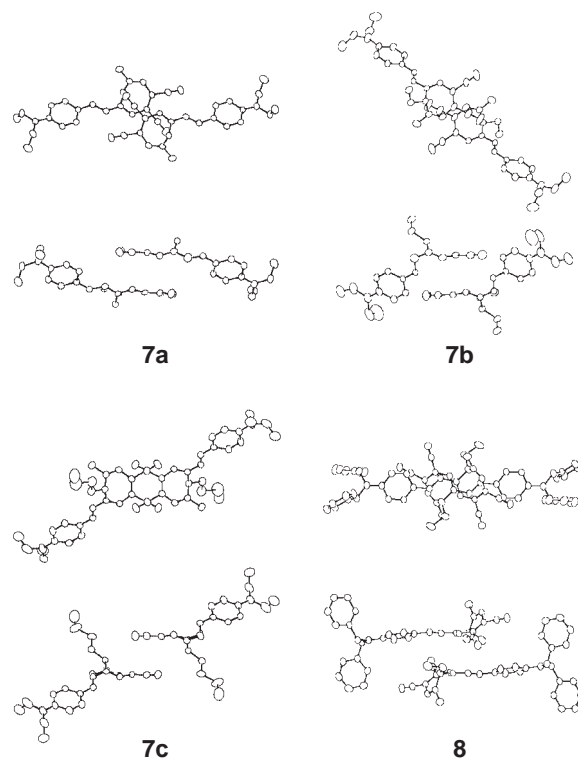


Fig. 5. Stacking pairs of **7a**, **7b**, **7c**, and **8** between dicyanodiazepine moieties.

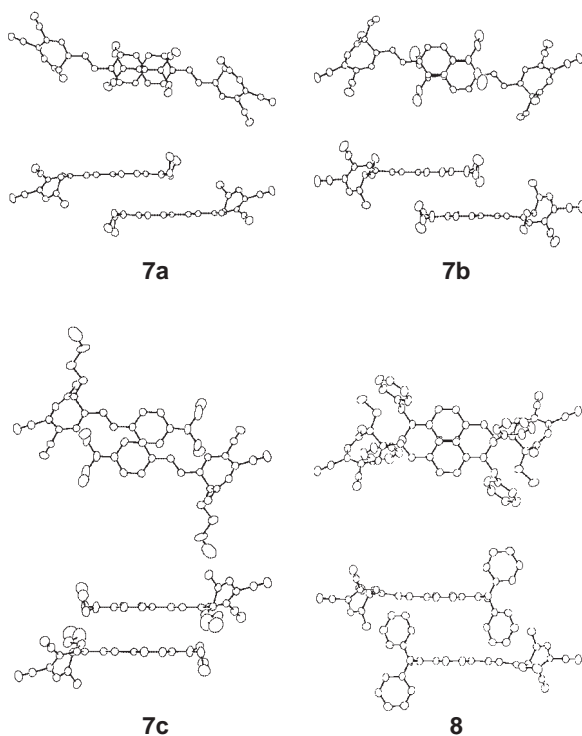


Fig. 4. Stacking pairs of **7a**, **7b**, **7c**, and **8** between phenylene rings.

rings. Two molecules are stacked in a tail-to-tail fashion. The interplanar distances between the phenylene rings were calculated to be 3.636, 3.832, 3.415, and 5.235 Å for **7a**, **7b**, **7c**, and

8, respectively. In compounds **7a**, **7b**, and **7c**, the longest interplanar distance was observed in the case of **7b**. This is ascribed to a different conformation of the diethylamino group compared to those of **7a** and **7c**. The ethyl groups of **7a** and **7c** point to the same direction; whereas those of **7b** are directed towards opposite directions. Because phenylene rings of **7c** are less overlapped than those of **7a** and **7b**, the repulsive interactions between the planes would be small to give the shortest interplanar distance. On the other hand, the distance in **8** is found to be considerably large. This must be due to the introduction of bulky substituents on the amino group.

Figure 5 illustrates the stacking pairs between the dicyanodiazepine moieties. The interplanar distance between planes composed of the dicyanoethene moiety in the dicyanodiazepine moieties were close: 3.389, 3.325, and 3.400 Å for **7a**, **7b**, and **7c**, respectively. The relative geometry for **8** was obtained to be 3.564 Å by calculating the interplanar distance between a plane composed of a part of the diazepine ring and the ethene moiety of the styryl group. No significant difference was observed among them, as compared with the case in the stacking pairs between phenylene rings. Close intermolecular atomic contacts were found between the nitrogen atoms of the diazepine ring and the carbon atoms in the dicyanoethene moiety in **7a** and **7b**. The cyano groups were closely stacked to each other in **7c**. These results indicate that the electrostatic interactions should dominate the formation of this kind of stacking pairs. On the other hand, cyano groups showed no influence on the stacking pair in **8**, and there existed no significant intermolecular atomic contact. Hence, van der Waals interactions would be important in this case.

A molecular pair stacked in a head-to-tail fashion was also

recognized in **7a**, as shown in Fig. 6. The chromophores were found to be completely overlapped and to be closely stacked on each other. The interplanar distance was 3.257 Å. This type of pair was not observed for other derivatives. Because the methylene groups at the 6-position in the diazepine ring are directed to another molecule, the alkyl groups at the 6-position must inhibit this type of stacking. The fluorescence intensity of **7a** in vapor-deposited films is considerably weak compared to those of the others. From a structural point of view, this molecular pair is regarded as being a key structure for fluorescence intensity in the solid state. The stacking between π -conjugation systems, i.e. chromophores, is known to play a significant role in the fluorescence properties in the solid state.⁸

However, the actual influence of the interactions between molecules on the fluorescence properties has not been fully understood. On the other hand, the electronic states of a parallel dimer and H-aggregates have been successfully interpreted by a theoretical treatment based on quantum chemistry.¹¹ The parallel dimer and the related assemblies are generally non-fluorescent. In the case of **7a**, the excitation energies in the solid state would be quenched by a cofacial stacking pair to show weak fluorescence. Dye **7d** also exhibited very weak fluorescence in vapor-deposited films. One of the reason for this is the relatively weak fluorescence of **7d** in a solution. However, there also exists the possibility that **7d** may form a similar type

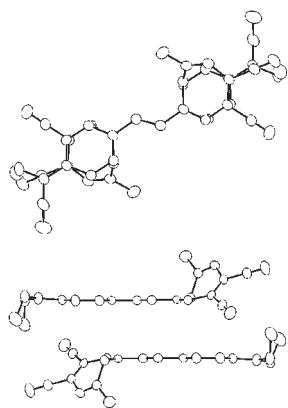


Fig. 6. Stacking pair of **7a** between whole chromophores.

of stacking pair, as shown in Fig. 6. The complete overlap between π -conjugation systems in a crystalline state is considered to be a key structure for evaluating the fluorescence properties in the solid state. Regulation of this type of stacking should be an effective strategy for enhancing the fluorescence intensity in the solid state.

Spectral Shift in Absorption. In the present dyes, substituents R^1 and R^2 are not directly correlated with the π -conjugation system. Therefore, the electronic structures of a molecule are almost similar, except for **7d**, because of the difference in an isomeric structure, as described in the next section. The similarity of the electronic structures was confirmed by semi-empirical molecular orbital calculations, as shown in Table 2.¹² No remarkable differences in λ_{\max} , f , and the HOMO and LUMO energy levels among **7a–d**, **8**, and **9** were calculated. Thus, the relative difference in the fluorescence intensity is considered to originate from the introduction of substituents. On the other hand, there exists a slight spectral shift in the absorption spectra from solution to the solid state. One of the reasons is an energy shift based on non-resonance interactions.¹¹ We also recognized that the effect of molecular deformation due to crystallization should not be neglected. This effect is one of the well-known intermolecular interactions showing an influence on the electronic states in the solid state. Organic molecules are generally deformed by crystallization to change the electronic states of molecules. Many examples of color polymorphism have been successfully explained by this effect.¹³ In the present study, this effect was found to contribute to a slight bathochromic shift from solution to the solid state, as shown in Table 3. The other well-known intermolecular interaction in the solid state is a resonance interaction in the excited states (exciton interaction).¹¹ In the present dyes, however, the nearest-neighboring molecules are aligned in such a way that the transition dipole moment in the visible region is arranged in an out-of-phase orientation. This state is symmetrically forbidden to give no optical transition. Thus, the two effects, that is the non-resonance interactions and the effect of deformation, can contribute to the spectral shift in these dyes from solution to the solid state.

Isomeric Structures of Dyes. The *axial*- and *equatorial*-isomers can exist for **7b**, **7c**, **7d**, **8**, and **9**. Because the *axial*-

Table 2. Calculated UV–vis Absorption Band for the Optimized Structure of Possible Isomers for **7a–d**, **8**, and **9**^{a)}

Compd	Conformation	λ_{\max}/nm	$f^{\text{b)}}$	HOMO/eV	LUMO/eV
7a ^{c)}	—	344.17	1.16	−7.5029	−0.8308
7b ^{c)}	<i>equatorial</i>	349.04	1.22	−7.3927	−0.7811
7b ^{d)}	<i>axial</i>	362.26	1.18	−7.4256	−0.8995
7c ^{c)}	<i>equatorial</i>	348.36	1.21	−7.4134	−0.7446
7c ^{d)}	<i>axial</i>	360.15	1.16	−7.4331	−0.8839
7d ^{d)}	<i>equatorial</i>	347.75	1.17	−7.4399	−0.7735
7d ^{c)}	<i>axial</i>	361.94	1.10	−7.4232	−0.9001
8 ^{c)}	<i>equatorial</i>	348.74	1.42	−7.3464	−0.7706
8 ^{d)}	<i>axial</i>	360.67	1.37	−7.3599	−0.9073
9 ^{c)}	<i>equatorial</i>	349.79	1.42	−7.2917	−0.7418
9 ^{d)}	<i>axial</i>	360.87	1.37	−7.3092	−0.8777

a) Calculated for *R*-isomers. b) Oscillator strength. c) Preferentially produced. d) Not detected.

Table 3. Calculated UV-vis Absorption Band for **7a–c** and **8** Using the Fractional Coordinate Sets of X-ray Analysis

Compd	Conformation	λ_{\max}/nm	f^{a}	HOMO/eV	LUMO/eV
7a	<i>equatorial</i>	356.62	1.31	−7.3027	−0.7988
7b	<i>equatorial</i>	357.73	1.22	−7.2184	−0.6505
7c	<i>equatorial</i>	370.52	1.30	−7.1333	−0.7101
8	<i>equatorial</i>	360.98	1.52	−7.1231	−0.6422

a) Oscillator strength.

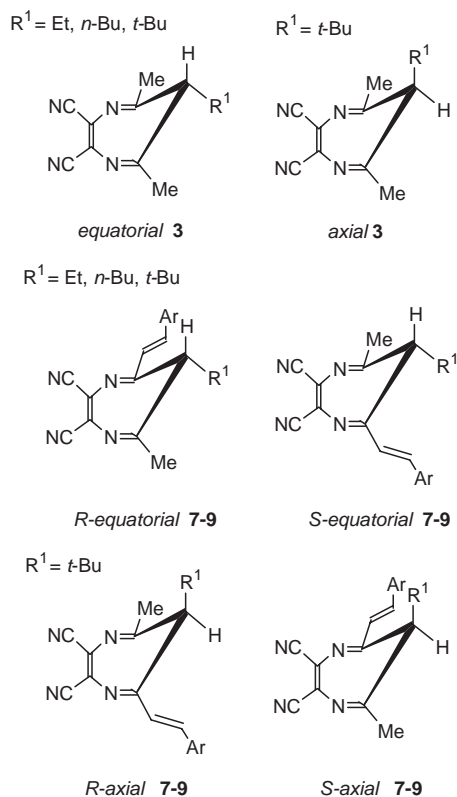


Fig. 7. Isomeric structures.

and *equatorial*-protons at the 6-position in diazepine ring can be distinguished by ^1H NMR spectroscopy, the isomers have been identified.¹⁴ Furthermore, since these compounds have an asymmetric carbon at the 6-position, the *R*- and *S*-isomers, whose UV-vis absorption and fluorescence spectra are identical, can also exist. Therefore, four kinds of isomers, as shown in Fig. 7, can exist for **7b**, **7c**, **7d**, **8**, and **9**. The ^1H NMR spectra of **3b** and **3c** showed that only the *equatorial-3* were formed. The ethyl and butyl substituted *equatorial-3* are more stable than the *axial-3* due to a steric repulsion between the alkyl group and the diazahexene moiety. Actually, the ^1H NMR spectra of **7b**, **7c**, **8**, and **9** in CDCl_3 indicated that only the *equatorial*-isomers existed in solution. The formations of *R*- and *S*-*equatorial 7b*, **7c**, and **8** were confirmed by X-ray structure analysis. Meanwhile, the ^1H NMR spectrum of **3d** in CDCl_3 showed that both the *equatorial*- and *axial-3d* were formed in a molar ratio of 3 to 2. The bulky *t*-butyl group can show a steric repulsion for the methyl groups at the 5- and 7-positions to produce both the *equatorial*- and *axial-3d*. Then, *equatorial*- and *axial-3d* can form *R-equatorial*, *S-equatorial*, *R-axial*, and *S-axial-7d*. However, interestingly, the

^1H NMR spectra of **7d** showed that only *axial-7d* were formed. This result can be attributed to the bulky *equatorial t*-butyl group adjacent to the methyl groups to inhibit the aldol reaction to preferentially give *axial-7d*. The molecular-orbital calculations for the *equatorial*- and *axial*-isomers revealed that the UV-vis absorption spectra of the *axial*-isomers exhibited a bathochromic shift of about 10–20 nm, compared with those of the related *equatorial*-isomers, as shown in Table 2. Thus, the bathochromicity of λ_{\max} and F_{\max} in **7d**, in which only the *axial*-isomers were produced, compared with those of **7b**, **7c**, **8**, and **9**, in which the *equatorial*-isomers were preferentially provided, is attributed to stabilization of the LUMO energy level.

Conclusion

The fluorescence intensity of novel nonplanar 2,3-dicyano-5-[4-(dialkylamino)styryl]-7-methyl-6*H*-1,4-diazepines in the solid state increased by introducing bulky substituents at the 6-position and the dialkylamino moiety, respectively, due to the prevention of a complete overlap between the chromophores. This structural feature is regarded as being the key structure for solid state fluorescence, and thus a modification of the molecular structure based on the present strategy should be effective to develop of emitters for non-doped EL displays.

Experimental

Instruments. Melting points were measured with a Yanagimoto MP-S2 micro-melting-point apparatus. EIMS spectra were recorded on a Shimadzu QP-1000 spectrometer. NMR spectra were obtained by a Varian Inova 400 spectrometer. Elemental analysis was performed with a Yanaco MT-6 CHN coder. UV-vis absorption and fluorescence spectra were taken on Hitachi U-3500 and F-4500 spectrophotometers, respectively. The fluorescence quantum yield was determined using quinine sulfate in 0.1 mol dm^{-3} sulfuric acid as a reference ($\Phi_f = 0.55$, $\lambda_{\text{em}} = 366$ nm). Vapor-deposited films were prepared by a conventional vacuum deposition equipment (ULVAC VPC-60) on a slide glass. The film thickness was measured with a Kosaka Laboratory Ltd., Surfcoorder SE-2300 Instrument.

Materials. DAMN (**1**) was purchased from Sigma-Aldrich. 4-(Diethylamino)benzaldehyde (**4**) were purchased from Tokyo Kasei Co., Ltd. 3-Ethylpentane-2,4-dione (**2b**) was purchased from Wako Pure Chemical Industries, Ltd. 1-Bromomethyl-3,5-di-*t*-butylbenzene,¹⁵ 3-butylpentane-2,4-dione (**2c**),¹⁶ 3-*t*-butyl-2,4-pentanedione (**2d**),¹⁷ and 2,3-dicyano-6*H*-1,4-diazepine (**3a**)¹⁴ were prepared as described in the literature.

Synthesis of *N,N*-dibenzyl- and *N,N*-bis(3,5-di-*t*-butylbenzyl)anilines. To a DMF solution (10 cm^3) of aniline (465 mg, 5 mmol) were added triethylamine (1.31 g, 13 mmol) and benzyl bromide or 3,5-di-*t*-butylbenzyl bromide (13 mmol). The mixture was stirred at room temperature for 5 h. After the reaction

was completed, the mixture was poured into water, extracted with ethyl acetate, and dried over sodium sulfate. After removing the solvent, the product was isolated by column chromatography (SiO₂, hexane:ethyl acetate = 20:1). The physical and spectral data are given below.

***N,N*-Dibenzylaniline:** Yield 36%. oil. ¹H NMR (CDCl₃) δ 4.64 (s, 4H), 6.70 (t, *J* = 8.1 Hz, 1H), 6.74 (d, *J* = 8.1 Hz, 2H), 7.17 (t, *J* = 8.1 Hz, 2H), 7.24–7.32 (m, 10H). EIMS (70 eV) *m/z* (rel intensity) 273 (M⁺; 34), 196 (16), 182 (19), 91 (100), 77 (25), 65 (21).

***N,N*-Bis(3,5-di-*t*-butylbenzyl)aniline:** Yield 25%. oil. ¹H NMR (CDCl₃) δ 1.22–1.33 (m, 36H), 4.60 (s, 4H), 6.69 (t, *J* = 8.0 Hz, 1H), 6.81 (d, *J* = 8.0 Hz, 2H), 7.10 (d, *J* = 1.8 Hz, 4H), 7.17 (t, *J* = 8.0 Hz, 2H), 7.29 (t, *J* = 1.8 Hz, 2H). EIMS (70 eV) *m/z* (rel intensity) 497 (M⁺; 34), 294 (98), 203 (58), 148 (43), 133 (49), 57 (100).

Synthesis of 6-Substituted 2,3-Dicyano-5,7-dimethyl-6*H*-1,4-diazepines 3. To a benzene solution (20 cm³) of DAMN (**1**, 1.08 g, 10 mmol) were added oxalic acid (50 mg, 0.6 mmol) and pentane-2,4-diones (**2**, 10 mmol). The mixture was refluxed for 5–31 h using a Dean–Stark trap. After removing the solvent, the product was isolated by column chromatography (SiO₂, **3b**; ethyl acetate, **3c**; ethyl acetate:hexane = 5:1, **3d**; dichloromethane) and recrystallized from benzene. The physical and spectral data are given below.

2,3-Dicyano-6-ethyl-5,7-dimethyl-6*H*-1,4-diazepine (3b): Yield 51%. mp 180–182 °C. ¹H NMR (CDCl₃) δ 1.51 (t, *J* = 7.4 Hz, 3H), 1.27 (t, *J* = 7.4 Hz, 1H), 2.15 (s, 6H), 2.21–2.36 (m, 2H). EIMS (70 eV) *m/z* (rel intensity) 200 (M⁺; 77), 185 (100).

6-Butyl-2,3-dicyano-5,7-dimethyl-6*H*-1,4-diazepine (3c): Yield 20%. mp 122–124 °C. ¹H NMR (CDCl₃) δ 0.99 (t, *J* = 7.0 Hz, 3H), 1.32 (t, *J* = 7.5 Hz, 1H), 1.42–1.46 (m, 4H), 2.13 (s, 6H), 2.22 (q, *J* = 7.5 Hz, 2H). EIMS (70 eV) *m/z* (rel intensity) 228 (M⁺; 51), 186 (44), 185 (83), 172 (52), 171 (50), 55 (100).

6-*t*-Butyl-2,3-dicyano-5,7-dimethyl-6*H*-1,4-diazepine (3d): Yield 8%. mp 160–162 °C. ¹H NMR (CDCl₃) δ 0.84 (s, 1H),* 1.32 (s, 9H),* 2.25 (s, 6H),* 0.98 (s, 9H),** 2.31 (s, 6H),** 4.08 (s, 1H)**. EIMS (70 eV) *m/z* (rel intensity) 228 (M⁺; 12), 213 (12), 172 (76), 57 (100), 41 (82). * and ** show the peaks attributed to the *equatorial*- and the *axial*-isomers, respectively.

Synthesis of 4-(Dialkylamino)benzaldehydes 5 and 6. To a DMF solution (2 cm³) of dialkylanilines (2 mmol) was added dropwise a DMF solution (1 cm³) of phosphorus trichloride (367 mg, 2.2 mmol), and allowed to stand at 0 °C. The mixture was stirred for 15 h at room temperature, then heated to 60 °C until the reaction was complete. The reaction mixture was poured into water, alkalized, and extracted with dichloromethane. After evaporating the solvent, the product was isolated by column chromatography (SiO₂, chloroform). The physical and spectral data are given below.

4-(Dibenzylamino)benzaldehyde (5): Yield 66%. mp 95–96 °C. ¹H NMR (CDCl₃) δ 4.75 (s, 4H), 6.79 (d, *J* = 8.8 Hz, 2H), 7.21–7.38 (m, 10H), 7.69 (d, *J* = 8.8 Hz, 2H), 9.73 (s, 1H). EIMS (70 eV) *m/z* (rel intensity) 301 (M⁺; 10), 210 (6), 91 (100), 65 (15).

4-[*N,N*-Bis(3,5-di-*t*-butylbenzyl)amino]benzaldehyde (6): Yield 69%. mp 130–133 °C. ¹H NMR (CDCl₃) δ 1.22–1.38 (m, 36H), 4.71 (s, 4H), 6.84 (d, *J* = 8.9 Hz, 2H), 7.02 (d, *J* = 1.8 Hz, 4H), 7.34 (t, *J* = 1.8 Hz, 2H), 7.71 (d, *J* = 8.9 Hz, 2H), 9.34 (s, 1H). EIMS (70 eV) *m/z* (rel intensity) 525 (M⁺; 40), 322 (70), 203 (54), 148 (70), 133 (53), 57 (100).

Synthesis of 2,3-Dicyano-5-methyl-6*H*-1,4-diazepine Dyes 7–9. To a benzene solution (15 cm³) of 6-substituted 2,3-dicyano-5,7-dimethyl-6*H*-1,4-diazepines **3** (1 mmol) were added piperidine (5 drops) and 4-(dialkylamino)benzaldehydes **4–6** (1 mmol). The mixture was stirred with a Dean–Stark trap (**7a**, **7b**, and **7c**; reflux, 6 h, **7d**; 50 °C to reflux, 66 h, **8** and **9**; 60 °C to reflux, 7 h). After removing the solvent, the product was isolated by column chromatography (SiO₂, **7a** and **7b**; chloroform:ethyl acetate = 10:1, **7c** and **8**; toluene:ethyl acetate = 10:1, **7d**; benzene:ethyl acetate = 15:1, **9**; toluene:ethyl acetate = 30:1) and recrystallized (**7a**; benzene, **7b** and **8**; toluene, **7c**; cyclohexane, **7d**; ethanol–water, **9**; hexane). The physical and spectral data are shown below.

2,3-Dicyano-5-[4-(diethylamino)styryl]-7-methyl-6*H*-1,4-diazepine (7a): Yield 50%. mp >300 °C. ¹H NMR (CDCl₃) δ 1.21 (t, *J* = 7.2 Hz, 6H), 1.59 (s, 3H), 1.83 (br s, 1H), 3.43 (q, *J* = 7.2 Hz, 4H), 4.57 (br s, 1H), 6.67 (d, *J* = 15.9 Hz, 1H), 6.68 (d, *J* = 8.7 Hz, 2H), 7.44 (d, *J* = 15.9 Hz, 1H), 7.45 (d, *J* = 8.7 Hz, 2H). EIMS (70 eV) *m/z* (rel intensity) 331 (M⁺; 57), 317 (85), 316 (100). Anal. Found: C, 72.52; H, 6.53; N, 21.38%. Calcd for C₂₀H₂₁N₅: C, 72.48; H, 6.39; N, 21.13%.

2,3-Dicyano-5-[4-(diethylamino)styryl]-6-ethyl-7-methyl-6*H*-1,4-diazepine (7b): Yield 23%. mp 196–198 °C. ¹H NMR (CDCl₃) δ 1.17 (t, *J* = 7.4 Hz, 3H), 1.21 (t, *J* = 7.1 Hz, 6H), 1.39 (t, *J* = 7.4 Hz, 1H), 2.05 (s, 3H), 2.31–2.42 (m, 2H), 3.43 (q, *J* = 7.1 Hz, 4H), 6.31 (d, *J* = 15.0 Hz, 1H), 6.64 (d, *J* = 8.8 Hz, 2H), 7.41 (d, *J* = 8.8 Hz, 2H), 7.68 (d, *J* = 15.0 Hz, 1H). EIMS (70 eV) *m/z* (rel intensity) 359 (M⁺; 81), 344 (100). Anal. Found: C, 73.58; H, 7.06; N, 19.27%. Calcd for C₂₂H₂₅N₅: C, 73.51; H, 7.01; N, 19.48%.

6-Butyl-2,3-dicyano-5-[4-(diethylamino)styryl]-7-methyl-6*H*-1,4-diazepine (7c): Yield 16%. mp 132–134 °C. ¹H NMR (CDCl₃) δ 1.00 (t, *J* = 7.0 Hz, 3H), 1.21 (t, *J* = 7.0 Hz, 6H), 1.27 (br s, 1H), 1.42–1.48 (m, 4H), 2.04 (s, 3H), 2.21–2.33 (m, 2H), 3.42 (q, *J* = 7.0 Hz, 4H), 6.30 (d, *J* = 15.0 Hz, 1H), 6.64 (d, *J* = 8.8 Hz, 2H), 7.42 (d, *J* = 8.8 Hz, 2H), 7.67 (d, *J* = 15.0 Hz, 1H). EIMS (70 eV) *m/z* (rel intensity) 387 (M⁺; 52), 372 (100). Anal. Found: C, 74.44; H, 7.56; N, 18.08%. Calcd for C₂₄H₂₉N₅: C, 74.38; H, 7.54; N, 18.07%.

6-*t*-Butyl-2,3-dicyano-5-[4-(diethylamino)styryl]-7-methyl-6*H*-1,4-diazepine (7d): Yield 16%. mp 87–90 °C. ¹H NMR (CDCl₃) δ 0.99 (s, 9H), 1.21 (t, *J* = 7.1 Hz, 6H), 2.27 (s, 3H), 3.43 (q, *J* = 7.1 Hz, 4H), 4.35 (s, 1H), 6.59 (d, *J* = 15.4 Hz, 1H), 6.65 (d, *J* = 9.0 Hz, 2H), 7.44 (d, *J* = 9.0 Hz, 2H), 7.50 (d, *J* = 15.4 Hz, 1H). EIMS (70 eV) *m/z* (rel intensity) 387 (M⁺; 76), 372 (82), 330 (100), 289 (31), 245 (34), 217 (35). Anal. Found: C, 74.99; H, 7.68; N, 17.74%. Calcd for C₂₄H₂₉N₅: C, 74.38; H, 7.54; N, 18.07%.

2,3-Dicyano-5-[4-(dibenzylamino)styryl]-6-ethyl-7-methyl-6*H*-1,4-diazepine (8): Yield 39%. mp 200–202 °C. ¹H NMR (CDCl₃) δ 1.15 (t, *J* = 7.3 Hz, 3H), 1.36 (t, *J* = 7.3 Hz, 1H), 2.03 (s, 3H), 2.30–2.37 (m, 2H), 4.73 (s, 4H), 6.32 (d, *J* = 15.0 Hz, 1H), 6.73 (d, *J* = 9.1 Hz, 2H), 7.20–7.37 (m, 10H), 7.38 (d, *J* = 9.1 Hz, 2H), 7.65 (d, *J* = 15.0 Hz, 1H). EIMS (70 eV) *m/z* (rel intensity) 483 (M⁺; 18), 392 (6), 91 (100). Anal. Found: C, 79.66; H, 6.33; N, 14.13%. Calcd for C₃₂H₂₉N₅: C, 79.47; H, 6.04; N, 14.48%.

5-[4-[Bis(3,5-di-*t*-butylbenzyl)amino]styryl]-2,3-dicyano-6-ethyl-7-methyl-6*H*-1,4-diazepine (9): Yield 27%. mp 133–135 °C. ¹H NMR (CDCl₃) δ 1.16 (t, *J* = 7.4 Hz, 3H), 1.27 (s, 36H), 1.38 (t, *J* = 7.4 Hz, 1H), 2.05 (s, 3H), 2.29–2.43 (m, 2H), 4.69 (s, 4H), 6.34 (d, *J* = 15.0 Hz, 1H), 6.79 (d, *J* = 8.8 Hz, 2H),

7.02 (s, 4H), 7.33 (s, 2H), 7.40 (d, $J = 8.8$ Hz, 2H), 7.69 (d, $J = 15.0$ Hz, 1H). EIMS (70 eV) m/z (rel intensity) 504 ($M^+ - (C_4H_9)_2C_6H_3CH_2$; 44), 203 (85), 148 (17), 133 (35), 91 (17), 57 (100). Anal. Found: C, 81.43; H, 8.68; N, 9.82%. Calcd for $C_{48}H_{61}N_5$: C, 81.42; H, 8.68; N, 9.89%.

X-ray Crystallography. Single crystals for dyes **7a**, **7b**, **7c**, and **8** were obtained by a solvent-diffusion method using hexane and chloroform. In all dyes, racemic crystals were obtained. The details of the X-ray analysis for **7a**, **7b**, and **7c** are reported in Ref. 10. The diffraction data for **8** were collected by a RIGAKU Raxis RAPID-F imaging-plate area detector using graphite monochromated Cu K α radiation ($\lambda = 1.54178$ Å). Crystal data for **8**: $C_{32}H_{29}N_5$, $M_w = 483.61$, triclinic, $P\bar{1}$, $Z = 2$, $a = 10.04(3)$, $b = 10.30(6)$, $c = 13.79(5)$ Å, $\alpha = 92.3(2)^\circ$, $\beta = 99.3(1)^\circ$, $\gamma = 104.3(2)^\circ$, $D_{\text{calcd}} = 1.181$ g cm $^{-3}$, $T = 296$ K, $F_{000} = 512$, $\mu = 5.54$ cm $^{-1}$, 11307 reflections were collected, 4363 unique ($R_{\text{int}} = 0.042$). The structure was solved by a direct method (SIR88)¹⁸ and refined by full-matrix least-squares calculations. 3268 observed ($I > 2\sigma(I)$), 364 parameters, $R_1 = 0.064$, $wR_2 = 0.090$, refinement on F , H atoms were located on the calculated position and not refined. All calculations were performed using the Crystal Structure 3.10 program package.¹⁹ Crystallographic data have been deposited at the CCDC, 12 Union Road, Cambridge CB2 1EZ, UK, and copies can be obtained on request, free of charge, by quoting the deposition numbers for **7a** (CCDC222683), **7b** (CCDC222682), **7c** (CCDC222681), and **8** (CCDC230160).

References

- 1 J. Shinar, "Organic Light-Emitting Devices," Springer-Verlag, New York, Berlin, Heidelberg (2004).
- 2 S. A. Odom, S. R. Parkin, and J. E. Anthony, *Org. Lett.*, **23**, 4245 (2003).
- 3 Y. Aso, T. Okai, Y. Kawaguchi, and T. Otsubo, *Chem. Lett.*, **2001**, 420.
- 4 a) S. Toguchi, Y. Morioka, H. Ishikawa, A. Oda, and E. Hasegawa, *Synth. Met.*, **111/112**, 57 (2000). b) M. Yoshida, A. Fujii, Y. Ohmori, and K. Yoshino, *Jpn. J. Appl. Phys.*, **35**, L397 (1996).
- 5 H.-C. Yeh, S.-J. Yeh, and C.-T. Chen, *Chem. Commun.*, **2003**, 2632.
- 6 H.-C. Yeh, L.-H. Chan, W.-C. Wu, and C.-T. Chen, *J. Mater. Chem.*, **14**, 1293 (2004).
- 7 S. H. Kim, S. H. Yoon, S. H. Kim, and E. M. Han, *Dyes Pigm.*, **64**, 45 (2005).
- 8 a) H. Langhals, T. Potrawa, H. Noth, and G. Linti, *Angew. Chem., Int. Ed. Engl.*, **28**, 478 (1989). b) K. Shirai, M. Matsuoka, and K. Fukunishi, *Dyes Pigm.*, **42**, 95 (1999). c) M. Brinkmann, G. Gadret, M. Muccini, C. Taliani, N. Masciocci, and A. Sironi, *J. Am. Chem. Soc.*, **122**, 5147 (2000). d) M. Levitus, G. Zepeda, H. Dang, C. Godinesz, T.-A. V. Khuong, K. Schemieder, and M. A. Garcis-Garibay, *J. Org. Chem.*, **66**, 3188 (2001). e) K. Hirano, S. Minakata, and M. Komatsu, *Bull. Chem. Soc. Jpn.*, **74**, 1567 (2001). f) K. Yoshida, Y. Ooyama, H. Miyazaki, and S. Watanabe, *J. Chem. Soc., Perkin Trans. 2*, **2002**, 700. g) K. Yoshida, Y. Ooyama, S. Tanikawa, and S. Watanabe, *J. Chem. Soc., Perkin Trans. 2*, **2002**, 708. h) Z. Fei, N. Kocher, J. Mohrschladt, H. Ihmels, and D. Stalke, *Angew. Chem., Int. Ed.*, **42**, 783 (2003). i) K. Shirai, M. Matsuoka, S. Matsumoto, and M. Shiro, *Dyes Pigm.*, **56**, 83 (2003). j) C.-T. Chen, C.-L. Chlang, Y.-C. Lin, L.-H. Chan, C.-H. Huang, Z.-W. Tsai, and C.-T. Chen, *Org. Lett.*, **5**, 1261 (2003). k) Y. Sonoda, Y. Kawanishi, T. Ikeda, M. Goto, S. Hayashi, Y. Yoshida, N. Tanigaki, and K. Yase, *J. Phys. Chem. B*, **107**, 3376 (2003).
- 9 a) E. Horiguchi, K. Shirai, M. Matsuoka, and M. Matsui, *Dyes Pigm.*, **53**, 45 (2002). b) E. Horiguchi, K. Shirai, J.-Y. Jung, M. Furusho, K. Takagi, and M. Matsuoka, *Dyes Pigm.*, **50**, 99 (2001).
- 10 E. Horiguchi, S. Matsumoto, K. Funabiki, and M. Matsui, *Chem. Lett.*, **33**, 170 (2004).
- 11 M. Kasha, "Spectroscopy of the Excited State," ed by B. D. Bartolo, Plenum Press, New York (1976), p. 337.
- 12 Win MOPAC ver. 3.0 package, Fujitsu, Chiba, Japan.
- 13 J. Bernstein, "Polymorphism in Molecular Crystals," Oxford University Press, New York (2002), and references cited therein.
- 14 R. W. Begland, D. R. Hartter, F. N. Joes, D. J. Sam, W. A. Sheppard, O. W. Webster, and F. J. Weigert, *J. Org. Chem.*, **39**, 2341 (1974).
- 15 K. R. Kopecky and M. Yeung, *Can. J. Chem.*, **66**, 374 (1988).
- 16 N. Ono, T. Yoshimura, T. Saito, R. Tamura, R. Tanigawa, and A. Kaji, *Bull. Chem. Soc. Jpn.*, **52**, 1716 (1979).
- 17 W. Jiao and T. D. Lash, *J. Org. Chem.*, **68**, 3896 (2003).
- 18 M. C. Burla, M. Camalli, G. Cascarano, C. Giacovazzo, G. Polidori, R. Spagna, and D. Viterbo, *J. Appl. Crystallogr.*, **22**, 389 (1989).
- 19 Crystal Structure 3.10: Crystal Structure Analysis Package, Rigaku and Rigaku/MS (2000–2002).